nanoenergy advances

Article

Continuously Interconnected N-Doped Porous Carbon for High-Performance Lithium-Ion Capacitors

Qing Wang [1], Xin Jiang [1], Qijun Tong [1], Haijian Li [2], Jie Li [2] and Weiqing Yang [1,*]

[1] Key Laboratory of Advanced Technologies of Materials, Ministry of Education, School of Materials Science and Engineering, Southwest Jiaotong University, Chengdu 610031, China
[2] Jinshi Technology Co. Ltd., 289 Longquanyi District, Chengdu 610100, China
* Correspondence: wqyang@swjtu.edu.cn

1. Supplementary Materials

Figure. S1 Typical SEM images of the porous carbon showing the smooth and discontinuous pore structure.

Figure. S2 Typical TEM images of the porous carbon (PC) and N-doped porous carbon (N−PC).

Figure. S3 Physical characterizations of PC and N−PC.

Figure. S4 TEM images of the Nb2O5 prepared at different reactive temperatures.

Figure. S5 Typical SEM images of N-PC with three-dimensional skeleton structure and rough surface.

Figure. S6 Raman spectrum of PC and N−PC.

Figure. S7 SEM images of the Nb2O5 prepared at different reactive temperatures.

Figure. S8 Physical characterizations of PC and N−PC.

Figure. S9 CV curves of a) PC and b) N-PC at different scan rates.

Figure. S10 Electrochemical properties of N−PC cathode.

Figure. S11 Electrochemical properties of Nb2O5-600, Nb2O5-700 and Nb2O5-800.

Table S1 Analysis of the fitted N1s peaks from XPS.

Table S2 Analysis of the fitted C1s peaks from XPS.

Table S3 Analysis of the fitted O1s peaks from XPS.

Table S4 Porosity parameters of PC and N−PC.

Citation: Wang, Q.; Jiang, X.; Tong, Q.; Li, H.; Li, J.; Yang, W. Continuously Interconnected N-Doped Porous Carbon for High-Performance Lithium-Ion Capacitors. *Nanoenergy Adv.* **2022**, *2*, 303−315. https://doi.org/10.3390/nanoenergyadv2040016

Academic Editors: Kwang-Sun Ryu, Ya Yang

Received: 18 September 2022
Accepted: 24 October 2022
Published: 1 November 2022

2. Supplementary Figures

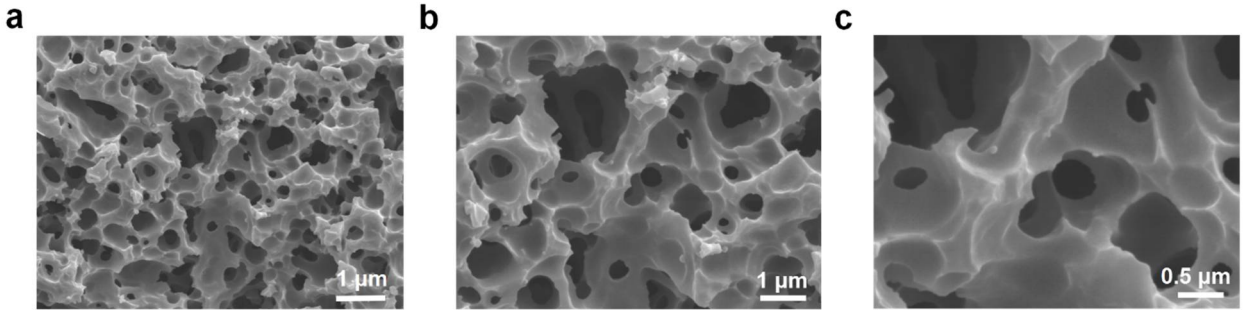

Figure S1. Typical SEM images of the porous carbon showing the smooth and discontinuous pore structure.

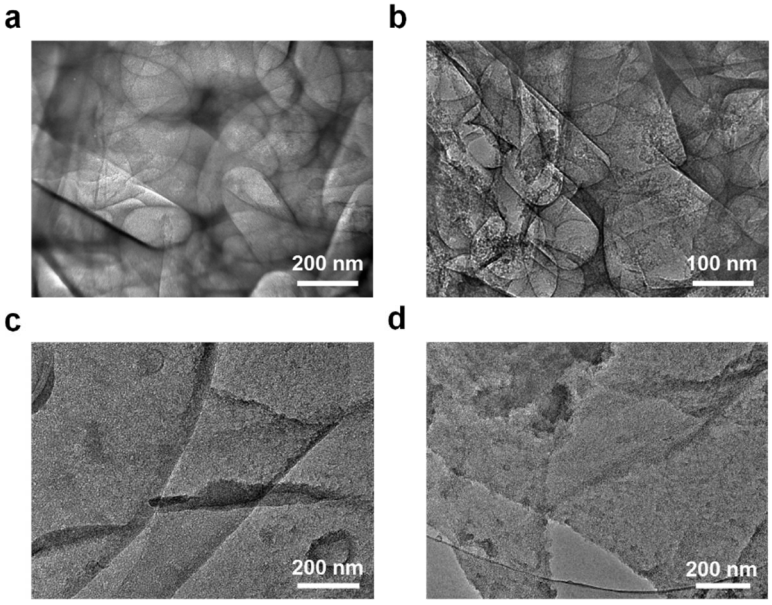

Figure S2. Typical TEM images of the porous carbon (PC) and N-doped porous carbon (N–PC). (**a**,**b**) TEM images of the porous carbon showing the smooth surface and porous structure. (**c**,**d**) TEM images of the N-doped porous carbon showing the lamellar structure with abundant defects.

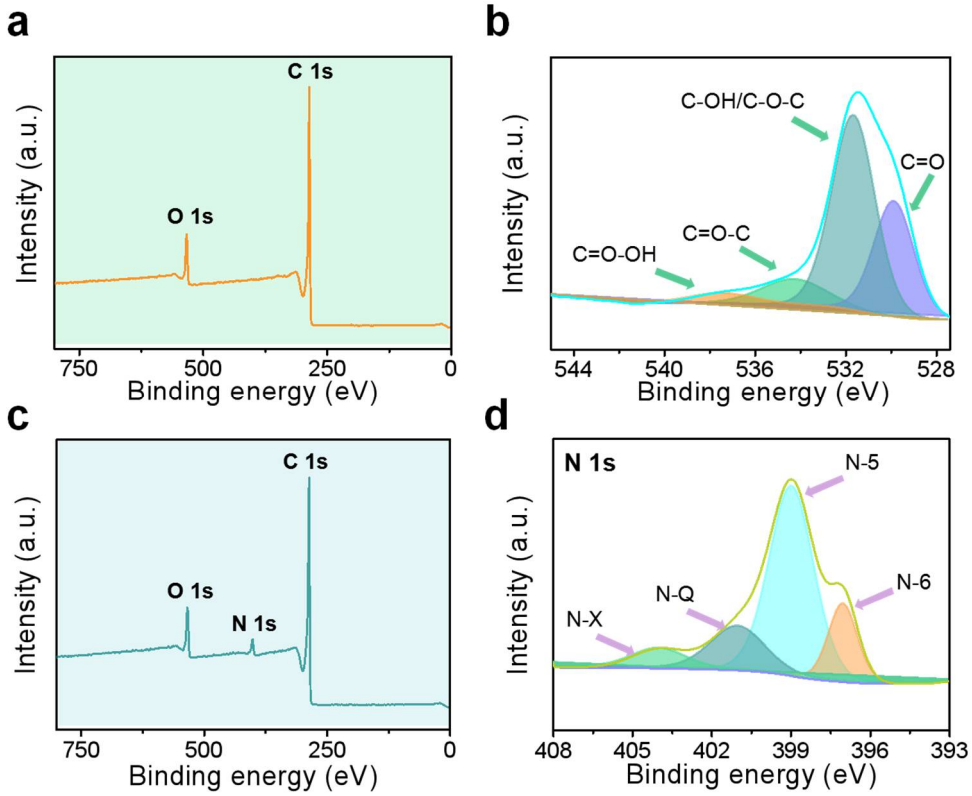

Figure S3. Physical characterizations of PC and N−PC. (**a**) XPS survey of PC. (**b**) Deconvolution curves of O1s of PC. (**c**) XPS survey of N−PC. (**d**) Deconvolution curves of N1s of N−PC.

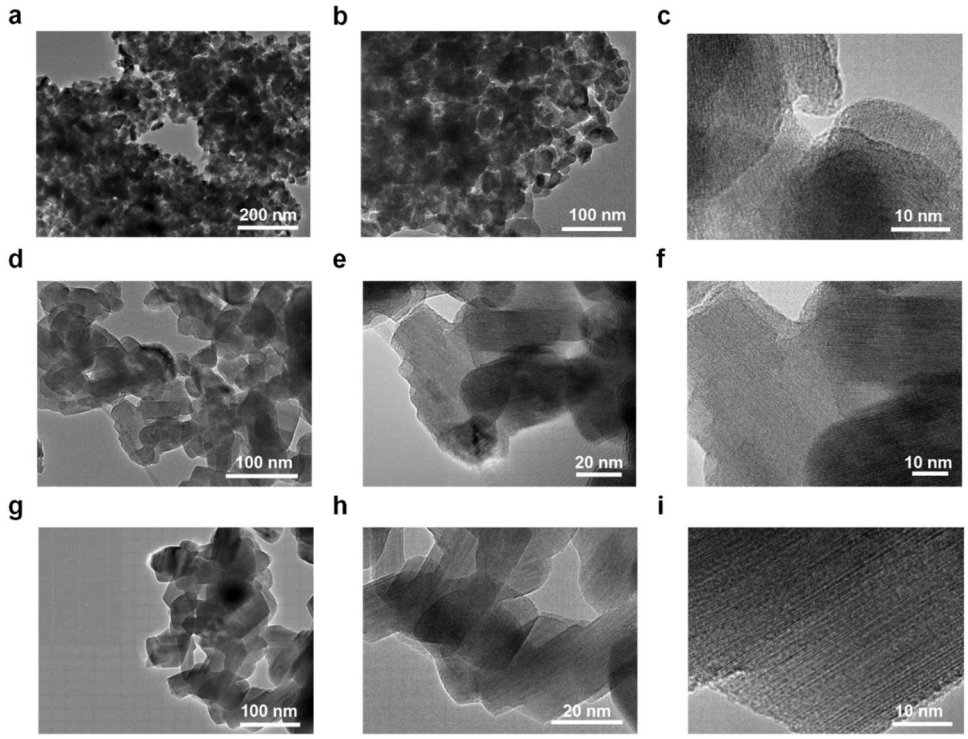

Figure S4. TEM images of the Nb_2O_5 prepared at different reactive temperatures (600 °C, 700 °C and 800 °C, name the Nb_2O_5-600, Nb_2O_5-700 and Nb_2O_5-800 respectively). (**a**,**b**) Low-resolution TEM images of Nb_2O_5-600 showing the dense particles. (**c**) High-resolution TEM image of Nb_2O_5-600. (**d**,**e**) Low-resolution TEM images of Nb_2O_5-700 showing the spherical structure. (**f**) High-resolution TEM image of Nb_2O_5-700. (**g**,**h**) Low-resolution TEM images of Nb_2O_5-800 showing the rectangular structure. (**i**) High-resolution TEM image of Nb_2O_5-700.

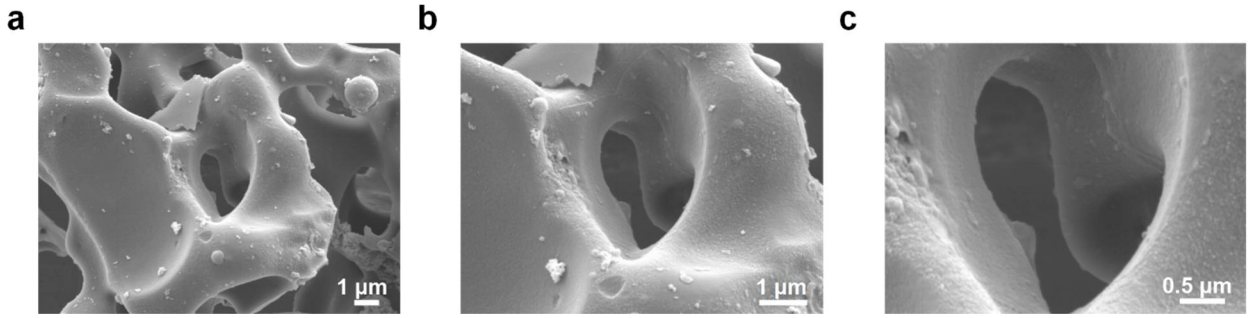

Figure S5. Typical SEM images of N–PC with three-dimensional skeleton structure and rough surface. Scale bars: 1 μm, 1 μm and 0.5 μm, respectively.

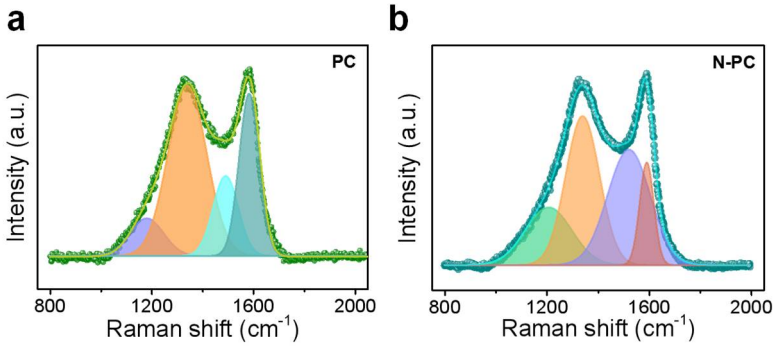

Figure S6. Raman spectrum of PC and N–PC.

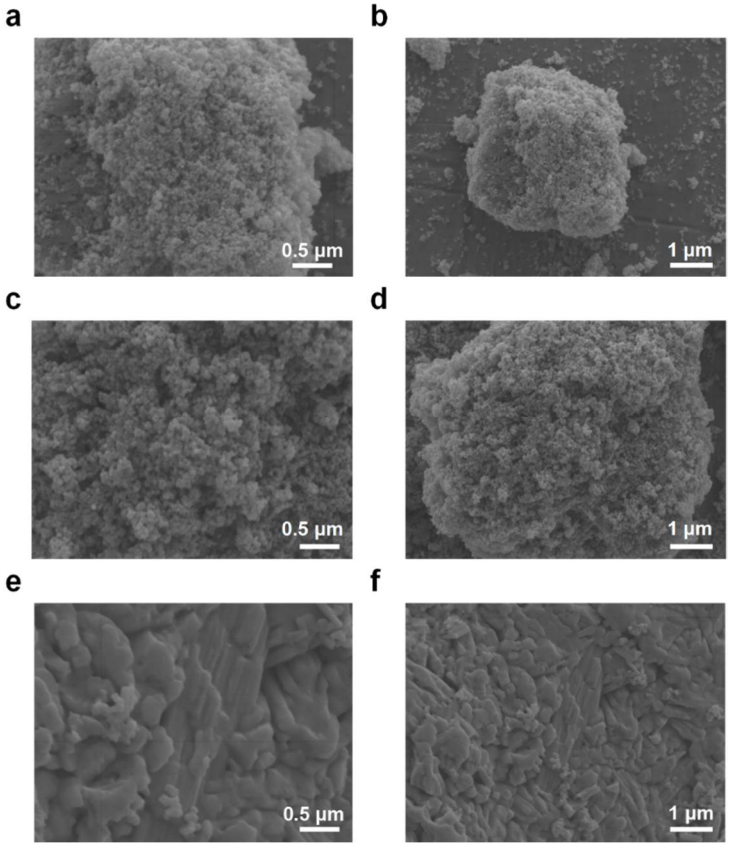

Figure S7. SEM images of the Nb_2O_5 prepared at different reactive temperatures (600 °C, 700 °C and 800 °C, name the Nb_2O_5-600, Nb_2O_5-700 and Nb_2O_5-800 respectively). (**a**) High-resolution SEM image of Nb_2O_5-600. Scale bar: 0.5 μm. (**b**) Low-resolution SEM image of Nb_2O_5-600. Scale bar: 1 μm.

(**c**) High-resolution SEM image of Nb_2O_5-700. Scale bar: 0.5 μm. (**d**) Low-resolution SEM image of Nb_2O_5-700. Scale bar: 1 μm. (**e**) High-resolution SEM image of Nb_2O_5-800. Scale bar: 0.5 μm. (**f**) Low-resolution SEM image of Nb_2O_5-800. Scale bar: 1 μm.

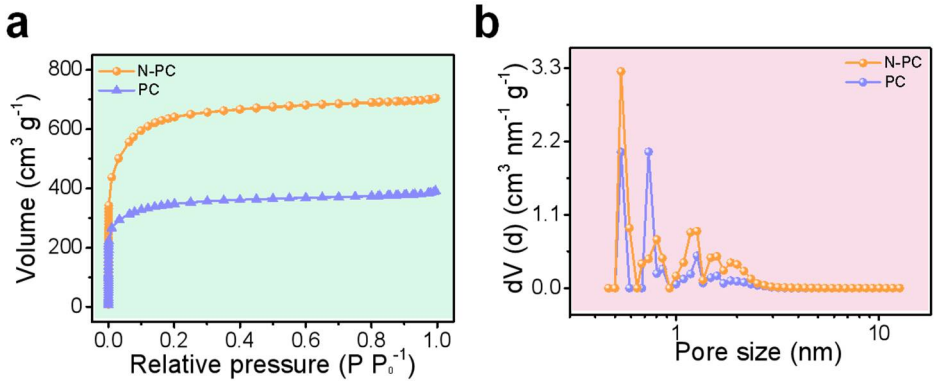

Figure S8. Physical characterizations of PC and N–PC. (**a**) N_2 adsorption/desorption isotherms. (**b**) Pore size distribution obtained using the density-functional theory (DFT) method.

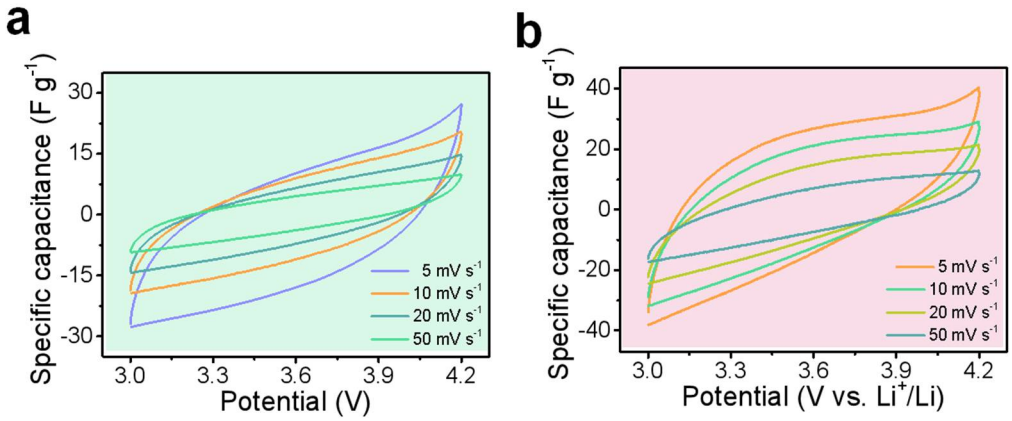

Figure S9. CV curves of (**a**) PC and (**b**) N–PC at different scan rates of 5–50 mV · s^{-1}.

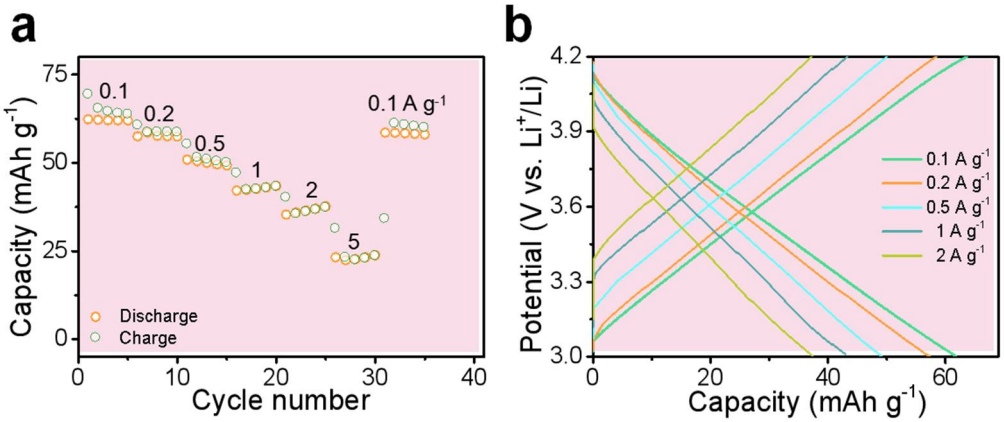

Figure S10. Electrochemical properties of N–PC cathode. (**a**) Rate performance of N–PC cathode. (**b**) GCD curves at different current densities.

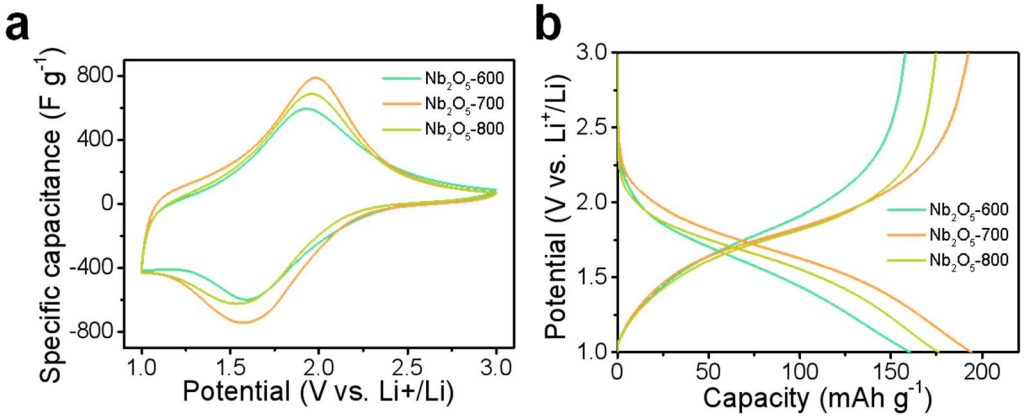

Figure S11. Electrochemical properties of Nb_2O_5-600, Nb_2O_5-700 and Nb_2O_5-800. (**a**) CV curve at a scan rate of 1 mV s^{-1}. (**b**) GCD curves at a current density of 0.1 A g^{-1}.

Table S1. Analysis of the fitted N1s peaks from XPS and their relative percentages of functional groups.

Samples	N 1s fitting binding energy (eV; relative percentage, %)			
	398.7 (N-6)	399.6 (N-5)	400.6 (N-Q)	402.0 (N-X)
N–PC	16.03	46.58	29.19	8.20

Table S2. Analysis of the fitted C1s peaks from XPS and their relative percentages of functional groups.

Samples	C 1s Fitting Binding Energy (eV; Relative Percentage, %)			
	284.80 (C-C/C=C)	285.77 (C-O)	288.18 (C=O)	291.10 (O-C=O)
PC	56.34	23.18	14.37	6.11
N–PC	47.96	27.05	17.15	7.84

Table S3. Analysis of the fitted O1s peaks from XPS and their relative percentages of functional groups.

Samples	O 1s Fitting Binding Energy (eV; Relative Percentage, %)			
	531.30 (C=O)	532.97 (C-O-C)	534.76 (O=C-O)	538.18 (COOH)
PC	28.22	57.22	10.42	4.14
N–PC	22.08	63.30	10.26	4.36

Table S4. Porosity parameters of PC and N-PC.

	N_2 Adsorption Desorption				
	SSA (m^2 g^{-1})			Pore Volume (cm^3 g^{-1})	
Sample	S_{BET} [a]	S_{micro} [b]	S_{ext} [c]	V_{total} [d]	V_{micro} [e]
PC	1306	874	431	0.60	0.34
N–PC	2419	1594	825	1.09	0.62

[a] Specific surface area (S_{BET}) was calculated using the Brunauer-Emmett-Teller (BET) method; [b,c] Specific micropore surface area (S_{micro}) and specific external surface area (S_{ext}) were calculated using the t-plot method; [d,e] The total pore volume (V_{total}) was determined at a relative pressure of 0.98, and the micropore volume (V_{micro}) was obtained by t-plot analysis.